

# Myristoylated PreS1-Domain of the Hepatitis B Virus L-protein Mediates Specific Binding to Differentiated Hepatocytes

Anja Meier,<sup>1</sup> Stefan Mehrle,<sup>1</sup> Thomas S. Weiss,<sup>2</sup> Walter Mier,<sup>3</sup> and Stephan Urban<sup>1</sup>

Chronic infection with the human hepatitis B virus (HBV) is a global health problem and a main cause of progressive liver diseases. HBV exhibits a narrow host range, replicating primarily in hepatocytes. Both host and hepatocyte specificity presumably involve specific receptor interactions on the target cell; however, direct evidence for this hypothesis is missing. Following the observation that HBV entry is specifically blocked by L-protein-derived preS1-lipopeptides, we visualized specific HBV receptor/ligand complexes on hepatic cells and quantified the turnover kinetics. Using fluorescein isothiocyanate-labeled, myristoylated HBV preS1-peptides we demonstrate (1) the presence of a highly specific HBV receptor on the plasma membrane of HBV-susceptible primary human and tupaia hepatocytes and HepaRG cells but also on hepatocytes from the nonsusceptible species mouse, rat, rabbit and dog; (2) the requirement of a differentiated state of the hepatocyte for specific preS1-binding; (3) the lack of detectable amounts of the receptor on HepG2 and HuH7 cells; (4) a slow receptor turnover at the hepatocyte membrane; and (5) an association of the receptor with actin microfilaments. The presence of the preS1-receptor in primary hepatocytes from some non-HBV-susceptible species indicates that the lack of susceptibility of these cells is owed to a postbinding step. **Conclusion:** These findings suggest that HBV hepatotropism is mediated by the highly selective expression of a yet unknown receptor\* on differentiated hepatocytes, while species specificity of the HBV infection requires selective downstream events, e.g., the presence of host dependency or the absence of host restriction factors. The criteria defined here will allow narrowing down reasonable receptor candidates and provide a binding assay for HBV-receptor expression screens in hepatic cells. (HEPATOLOGY 2013;58:31-42)

See Editorial on Page 9

Chronic hepatitis B is a global medical problem caused by the human hepatitis B virus (HBV). About 350 million people are persistently infected and need therapeutic treatment to reduce the risk of developing liver cirrhosis and HCC.<sup>1</sup> Since the

currently approved medications are mostly noncurative, novel therapeutic strategies are needed.<sup>2</sup>

HBV, the prototypic member of the hepadnavirus family, is a 42 nm, enveloped, partially double-stranded DNA virus with a restricted host range and an extraordinary tropism to infect the parenchymal liver cells of its host.<sup>3</sup> Since HBV properly assembles

Abbreviations: DIPEA, *N,N*-Diisopropylethylamine; DMSO, dimethyl sulfoxide; FITC, fluorescein isothiocyanate; *ge*, genome equivalent; HBTU, *O*-(benzotriazol-1-yl)-*N,N,N',N'*-tetramethyluronium hexafluorophosphate; HSPG, heparan sulfate proteoglycan; L-protein, hepatitis B virus large surface protein; PBS, phosphate-buffered saline; PEG, polyethylene glycol; PHH, primary human hepatocytes; PMH, primary mouse hepatocytes; PTH, primary Tupaia belangeri hepatocytes.

From the <sup>1</sup>Department of Infectious Diseases, Molecular Virology, University Hospital Heidelberg, Heidelberg, Germany; <sup>2</sup>Center for Liver Cell Research, Department of Pediatrics, University Medical Center Regensburg, Regensburg, Germany; <sup>3</sup>Department of Nuclear Medicine, University Hospital Heidelberg, Heidelberg, Germany

Received July 11, 2012; accepted November 6, 2012.

This work received grants from the Bundesministerium für Bildung und Forschung (BMBF), "Innovative Therapieverfahren," grant number 01GU0702, the Landesstiftung Baden Württemberg and financial support from the Vision 7 GmbH.

\*The data presented in this study is consistent with the recent publication of Yan et al. describing sodium taurocholate cotransporting polypeptide (NTCP/SLC10A1) as a specific receptor for HBV and HDV infection. Yan H, Zhong G, Xu G, He W, Jing Z, Gao Z, et al. Sodium taurocholate cotransporting polypeptide is a functional receptor for human hepatitis B and D virus. *elife* 2012;1:e00049.

after transfection with genomic HBV DNA of even nonhepatic cells, the specificity for hepatocytes must be related to an early infection event. One of the proposed restricted steps might be the lack of a hepatocyte-specific receptor. However, this hypothesis needs to be proven.

The envelope of HBV consists of proteins termed large (L), middle (M), and small (S) protein. They are encoded in one open reading frame and share the C-terminal S-domain which provides four trans-membrane helices<sup>4</sup> and is probably involved in fusion.<sup>5</sup> In addition to the S-domain, the M-protein contains an extension of 55 amino acids called preS2. The L-protein has a further N-terminal extension termed preS1. The preS1-domain of L- becomes N-terminally myristoylated and plays a key role in HBV entry into hepatocytes.<sup>6</sup>

Due to the previous limitation to primary human (PHHs) and primary tupaia belangeri hepatocytes (PTH) and HepaRG cell lines as the only *in vitro* HBV infection systems, receptor recognition and the mechanism of virus entry and membrane fusion are just about to be understood. Using HepaRG cells<sup>7</sup> and primary PTH,<sup>8</sup> heparin sulfate proteoglycans (HSPG) were identified as inevitable to initiate HBV infection.<sup>9,10</sup> Since HSPG interaction cannot explain HBV hepatocyte specificity, it is supposed an essential but not very specific step.

Using recombinant HBV and hepatitis delta virus (HDV) as a surrogate system to study HBV entry, essential infectivity determinants within the envelope proteins have been identified: (1) N-terminal myristoylation of L is mandatory for infectivity.<sup>11,12</sup> (2) Consecutive removal or insertion of short sequences in the N-terminal 75 amino acids (genotype D) of the preS1-domain abrogates infection.<sup>13,14</sup> Deletions and mutations introduced C-terminally of amino acid 75 including elimination of the M-protein and randomization of the preS2-domain within the L-protein had almost no influence on infectivity.<sup>15,16</sup> (3) Besides preS1, another essential element of HBV/HDV infectivity has been assigned to the antigenic loop (AGL) of the S-domain.<sup>17</sup> Replacement of cysteine residues in the AGL rendered HDV and HBV (Yi Ni, unpubl. results) noninfectious. Since some of these cysteines (e.g., Cys-124) participate in intramolecular disulfide

bonds, the sensitivity against reducing agents hints at the involvement of disulfide-bridge rearrangements during virus entry.<sup>18</sup> Since only L-protein containing SVPs are able to bind hepatocytes from *Tupaia belangeri* the S-protein/domain is probably not essential for hepatocyte-specific binding.<sup>19</sup>

Consistent with the results of the mutational analyses, HBV preS1-derived lipopeptides, mimicking the myristoylated N-terminal preS1-infectivity domain, efficiently inhibit HBV and HDV infection of HepaRG cells, PHH, and PTH.<sup>7,20-23</sup> The activity of the peptides requires myristoylation and the integrity of an internal sequence (9-NPLGFFP-15) which is highly conserved between primate hepadnaviruses.<sup>21</sup> Since their inhibitory effect remains for several hours after preincubation they probably inactivate a cellular receptor.<sup>24</sup>

In the present study we used fluorescently labeled, myristoylated HBVpreS1-peptides to analyze the presence and turnover kinetics of this HBVpreS1-specific receptor on hepatocytes from different species. We investigated whether receptor expression coincides with the species specificity of HBV and demonstrate highly specific binding of the preS1-lipopeptide to permissive cells (PHH, PTH, HepaRG). Unexpectedly, we detected specific binding to hepatocytes from non-susceptible species such as mouse, rat, rabbit, and dog, but not pig, cynomolgus, or rhesus monkey. Expression of a functional HBVpreS1-receptor was associated with the differentiation state of the hepatocyte: No binding was observed in undifferentiated HepaRG cells or dedifferentiated PMH and PHH. HepG2 and HuH7 cells were unable to bind the peptide even after dimethyl sulfoxide (DMSO)-induced differentiation. Kinetic studies demonstrated a slow turnover and a constrained lateral movement of the receptor complex at the plasma membrane (PM), possibly due to a cytoskeleton interaction.

## Materials and Methods

**Synthesis of Peptides.** Peptides were produced by solid phase synthesis employing the Fmoc/tBu strategy with O-(benzotriazol-1-yl)-N,N,N',N'-tetramethyluronium hexafluorophosphate; (HBTU) / N,N-Diisopropylethylamine (DIPEA) activation in an Applied Biosystems 433A peptide synthesizer. Fluorescein

Address reprint requests to: Prof. Dr. Stephan Urban, Department of Infectious Diseases, Molecular Virology, University Hospital Heidelberg, Im Neuenheimer Feld 345, D-69120 Heidelberg, Germany. E-mail: Stephan.Urban@med.uni-heidelberg.de; fax: +49-6221-561946.

Copyright © 2013 by the American Association for the Study of Liver Diseases.

View this article online at [wileyonlinelibrary.com](http://wileyonlinelibrary.com).

DOI 10.1002/hep.26181

Potential conflict of interest: Nothing to report.

Additional Supporting Information may be found in the online version of this article.

isothiocyanate (FITC; AppliChem) was coupled to the  $\epsilon$ -amino group of an introduced D-lysine at position 49. Alternatively, Atto-565-maleimide (Fluka) was linked to a cysteine at the same position. Reversed phase high-performance liquid chromatography (HPLC) was carried out as described (Schieck et al.<sup>25</sup>). The identity of the peptides was verified by mass spectrometry. Stock solutions (500  $\mu$ M) of the peptides in 2% DMSO were prepared, diluted with the appropriate medium, and added to the cells at the indicated concentrations.

**Preparation and Cultivation of Primary Hepatocytes and Cell Lines.** PHH were cultivated in serum-free medium as described.<sup>26</sup> Tissue samples from liver resections were obtained from patients undergoing partial hepatectomy. Experimental procedures were performed according to the guidelines of the charitable state controlled foundation HTCR (Human Tissue and Cell Research), with the informed patient's consent approved by the local Ethical Committee of the University of Regensburg. PMH were prepared by a two-step standard perfusion protocol using a 2-mM EGTA-containing buffer, followed by a treatment with 3.3 mg/mL collagenase type IV (Sigma-Aldrich).<sup>27</sup> Parenchymal cells were enriched through resuspension and centrifugation of the cells in a Percoll solution with a density of 1,063 g/mL. Cryopreserved hepatocytes were bought from Celsis (rabbit, dog, cynomolgus monkey, rhesus monkey, and pig) or BD Gentest (rat and cynomolgus monkey). Cryopreserved PTHs were a kind gift of Maura Dandri (Hamburg). HuH7 and HepG2 cell lines were cultivated in Dulbecco's modified Eagle's medium (DMEM), supplemented with 10% fetal calf serum (FCS), L-glutamine (2 mM), penicillin (50 U/mL), and streptomycin (50  $\mu$ g/mL). HepaRG cells were cultivated as described.<sup>7</sup> To induce differentiation, HuH7 and HepG2 cells were treated for 14 days with 0.5% DMSO; dedifferentiation of PMH and PHH was induced by growth in DMSO-free medium for up to 8 days.

**Binding Assays with Fluorescently Labeled HBVpreS-peptides.** Binding experiments were performed in supplemented Williams E medium as described above. For PHH, medium was complemented with 50  $\mu$ M hydrocortisone and 5  $\mu$ g/mL insulin. Experiments with primary hepatocytes were carried out either on day 1 after plating (microscopy) or immediately after thawing (flow cytometry). HepaRG cells were tested on day 5 after seeding, or 2 weeks after DMSO-induced differentiation. Cells were incubated at 37°C with the appropriate labeled peptide in medium. Binding competition was carried out

by coincubation of HBVpreS/2-48<sup>myr</sup>-K-FITC with an excess of unlabeled HBVpreS/2-48<sup>myr</sup>.

**Infection Inhibition.** For infection inhibition, HepaRG cells were preincubated for 30 minutes with peptide and inoculated with a 1:20 dilution of a polyethylene glycol (PEG)-precipitated (50- to 100-fold enrichment) HepG2.2.15/HepAd38-derived virus stock (16 hours at 37°C)<sup>7</sup> in medium containing 250 nM peptide and 4% PEG 8000 (Sigma-Aldrich). Cells were repeatedly washed and cultivated for up to 2 weeks. To quantify HBV replication, medium was collected from day 8 to 13 post infection and secreted HBeAg was determined by enzyme-linked immunosorbent assay (ELISA (AxSym, Abbott)).

**Fluorescence Microscopy.** Primary hepatocytes were grown on coverslips, coated with 0.1 mg/mL collagen (Cell Systems). After incubation with peptide at 37°C, cells were washed in phosphate-buffered saline (PBS), fixed (4% paraformaldehyde [PFA]), and mounted in DAPI-containing mounting medium (VectaShield). Microscopy was performed on a Perkin Elmer spinning disk confocal microscope, using a 60 $\times$  WI (NA 1.2) or 100 $\times$  oil (NA 1.4) objective, a Hamamatsu C9100-50 camera, and the software Velocity (Perkin Elmer). Quantification of peptide binding was achieved by measurement of the gray values in 60 (Fig. 5A) or 50 (Fig. 5B) circular selections in 3 or 10 representative pictures using ImageJ (NIH, Bethesda, MD). To analyze fluorescence recovery after photobleaching (FRAP), PMH were grown on collagen-coated chambered coverglass (LabTek). Cells were incubated with 400 nM HBVpreS/2-48<sup>myr</sup>-C-Atto565, diluted in Leiboviz (L-15) phenol red-free medium for 1 hour at 37°C, washed, and supplied with fresh L-15. As a control, cells were stained with 5  $\mu$ L/mL Vybrant DiI (Invitrogen). Live cell microscopy at 37°C was performed in a heated chamber. Bleaching was achieved using the 568 nm laser, and recovery of fluorescence was monitored for 30 seconds with a frequency of 2 frames per second.

**Flow Cytometry.** The  $4 \times 10^5$ /mL freshly prepared or cryopreserved primary hepatocytes were incubated for 30 minutes at room temperature with 200 nM of the respective peptide. After washing (PBS) flow cytometry was performed using a FACS Calibur and the software Cell Quest Pro (Becton-Dickinson). Competition of binding was performed with a 100-fold excess of unlabeled HBVpreS/2-48<sup>myr</sup> or control peptides (HBVpreS/2-48<sup>myr</sup>(D11,13) and HBVpreS/1-48). Cell viability was assessed by propidium iodide. To exclude unspecific binding caused by nonparenchymal cells,

hepatocyte preparations were controlled by uptake of acLDL (10  $\mu\text{g}/\text{mL}$  for 2 hours at 37°C), a marker for endothelial cells.

## Results

### *Fluorescently Labeled HBVpreS/2-48<sup>myr</sup> Specifically Binds to the PM of Hepatic HepaRG Cells.*

Myristoylated HBV-preS1 lipopeptides inhibit HBV infection of HepaRG cells.<sup>21</sup> To investigate specific receptor-interaction, we synthesized a fluorescently labeled variant of HBVpreS/2-48<sup>myr</sup> (Fig. 1A) and performed binding assays with HepaRG cells. Cosynthetic coupling of one FITC-moiety per molecule HBVpreS/2-48<sup>myr</sup>-K-FITC was accomplished by introduction of a lysine at position 49. As a control, we synthesized a mutant lipopeptide in which the L-leucine at position 11 and the L-phenylalanine at position 13 were replaced by the respective D-enantiomers (HBVpreS/2-48<sup>myr</sup>(D11,13)-K-FITC). A second control peptide comprised the wildtype sequence but lacked the N-terminal myristoyl moiety (HBVpreS/1-48-K-FITC). Both peptides are inactive (HBVpreS/2-48<sup>myr</sup>(D11,13)) or drastically impaired in inhibitory activity (HBVpreS/1-48).<sup>21</sup> To ensure that the K-FITC-residue had no effect on the inhibitory activity, we tested HBVpreS/2-48<sup>myr</sup>-K-FITC in comparison to the nonlabeled HBVpreS/2-48<sup>myr</sup> in an infection inhibition assay (Fig. 1B). HBVpreS/2-48<sup>myr</sup>-K-FITC inhibited HBV infection in PHH like HBVpreS/2-48<sup>myr</sup>, as measured by secreted HBeAg. HBVpreS/2-48<sup>myr</sup>(D11,13)-K-FITC was inactive, confirming the requirement of the 9-NPLGFFP-15 sequence. HBVpreS/1-48-K-FITC showed only marginal activity.

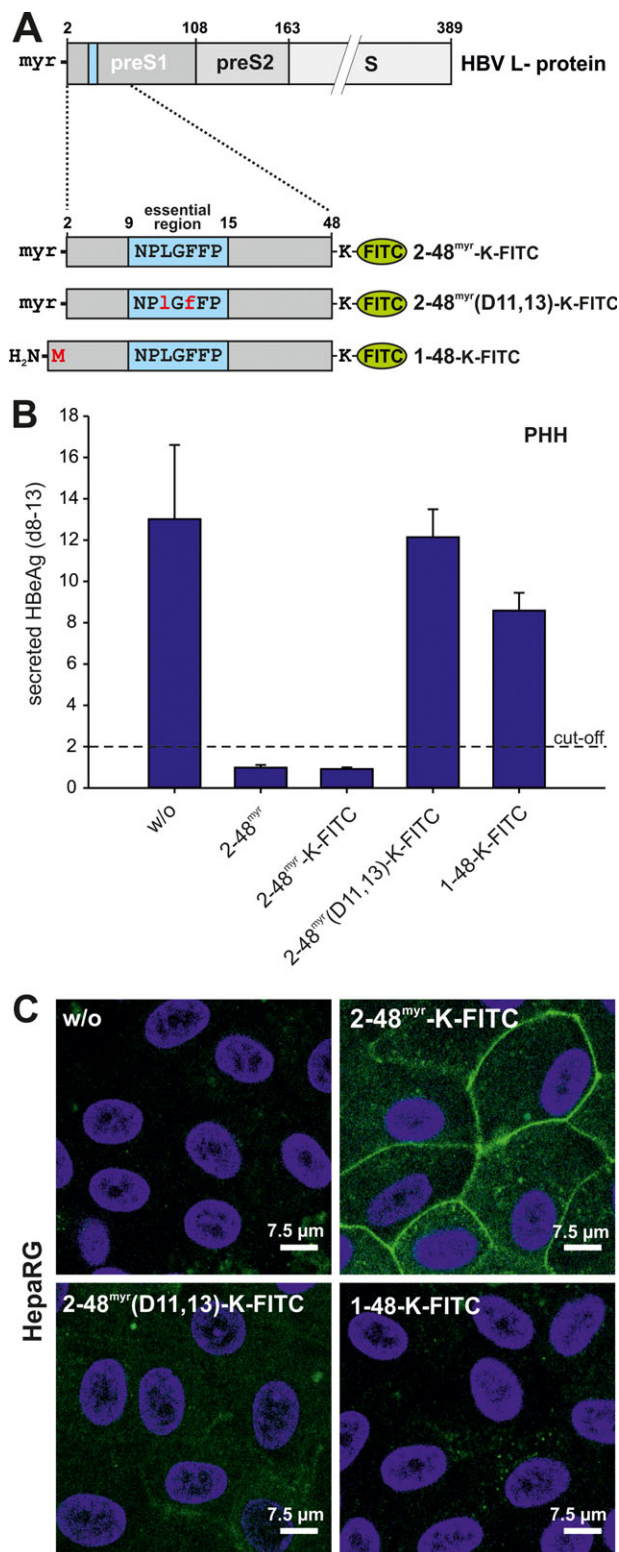


Fig. 1.

Fig. 1. HBVpreS/2-48<sup>myr</sup>-K-FITC inhibits HBV infection and specifically binds differentiated HepaRG cells. (A) Schematic representation of the HBV L-protein with its N-terminal myristic acid moiety (myr), the preS1, the preS2, and the S domain (above) in addition to the three fluorescently labeled peptides used in this study (below). HBVpreS/2-48<sup>myr</sup>-K-FITC (2-48<sup>myr</sup>-K-FITC) comprises the N-terminal 47 amino acids of the preS1-domain (genotype D) with the highly conserved essential domain 9-NPLGFFP-15 highlighted in blue. The peptide is N-terminally modified with myristic acid at glycine 2 and linked to an FITC-labeled lysine (K-FITC) at the C-terminus. HBVpreS/2-48<sup>myr</sup>(D11,13)-K-FITC (2-48<sup>myr</sup>(D11,13)-K-FITC), in which amino acids 11 and 13 were replaced by their respective D-enantiomers (shown by small capitals) and HBVpreS/1-48-K-FITC (1-48-K-FITC) which lacks N-terminal myristoylation, were used as controls. (B) HBV infection inhibition assay comparing the three fluorescently labeled peptides with HBVpreS/2-48<sup>myr</sup> (2-48<sup>myr</sup>). PHH were infected with a multiplicity of infection (MOI) of 10<sup>5</sup> GE/cell in the absence (w/o) or the presence of 250 nM unlabeled 2-48<sup>myr</sup> or labeled 2-48<sup>myr</sup>-K-FITC, 2-48<sup>myr</sup>(D11,13)-K-FITC and 1-48-K-FITC. Cell culture supernatants were collected between days 8 and 13 and secreted HBeAg (S/Co) was determined by ELISA. (C) Binding of fluorescently labeled peptides to HepaRG cells. Differentiated HepaRG cells were incubated with 200 nM of the respective peptide, washed, and fixed with 4% PFA. Images were obtained by confocal microscopy. Nuclei were stained with DAPI (blue), bound peptide is shown in green. Note that the cells in the absence of peptide (w/o) show autofluorescence within the cytoplasm but not at the plasma membrane.

To examine whether the differences in infection inhibition reflect specific binding properties to susceptible cells, we incubated differentiated HepaRG cells with the three peptides (200 nM) and analyzed cell association by confocal microscopy. As depicted in Fig. 1C, HBVpreS/2-48<sup>myr</sup>-K-FITC was localized at the PM of HepaRG cells (upper right). Incubation of cells with HBVpreS/2-48<sup>myr</sup>(D11,13)-K-FITC (lower left) or HBVpreS/1-48-K-FITC (lower right) did not result in significant PM staining, demonstrating the dependency of binding on the sequence integrity and the presence of the myristic acid. The specific peptide signal could clearly be discriminated from the punctuated

cellular autofluorescence detected in the absence of peptide (upper left). HBVpreS/2-48<sup>myr</sup>-K-FITC binding was observed only in the hepatic clusters of HepaRG cells but not in biliary cells (data not shown).

**HBVpreS/2-48<sup>myr</sup>-K-FITC Specifically Binds PHH and PTH.** Besides HepaRG cells, HBV infects PHH<sup>28</sup> and PTH<sup>8</sup> and is blocked by acylated HBVpreS-derived lipopeptides.<sup>20,24</sup> We therefore tested PHH and PTH for their ability to bind HBVpreS/2-48<sup>myr</sup>-K-FITC. We detected a sequence-specific and myristoyl-dependent association of the wildtype but not the control peptide with the PM of PHH (Fig. 2A). Specific binding of HBVpreS/2-48<sup>myr</sup>-K-FITC to PHH could also be detected in suspended cells by flow cytometry (Fig. 2B). Significant binding, visible by a shift of the cell population towards an approximately 10-fold higher fluorescence signal, was observed only for cells incubated with HBVpreS/2-48<sup>myr</sup>-K-FITC, but not with HBVpreS/2-48<sup>myr</sup>(D11,13)-K-FITC (Fig. 2B, dark green line versus orange line). Binding was prevented by an excess of the nonlabeled peptide HBVpreS/2-48<sup>myr</sup> (blue line) but not with the respective mutant HBVpreS/2-48<sup>myr</sup>(D11,13) (red line). This substantiates the high specificity of HBVpreS-receptor interaction in PHH. Consistently, PTH bound HBVpreS/2-48<sup>myr</sup>-K-FITC with comparable efficacy as PHH. Again, binding was prevented by unlabeled HBVpreS/2-48<sup>myr</sup> but not by the mutant HBVpreS/2-48<sup>myr</sup>(D11,13) (Fig. 2C).

**Binding of HBVpreS/2-48<sup>myr</sup>-K-FITC Is Not Restricted to HBV-Susceptible Hepatocytes.** To investigate if HBVpreS1-receptor expression is restricted to hepatocytes from HBV susceptible hosts, we performed binding studies using PMH that are not susceptible to

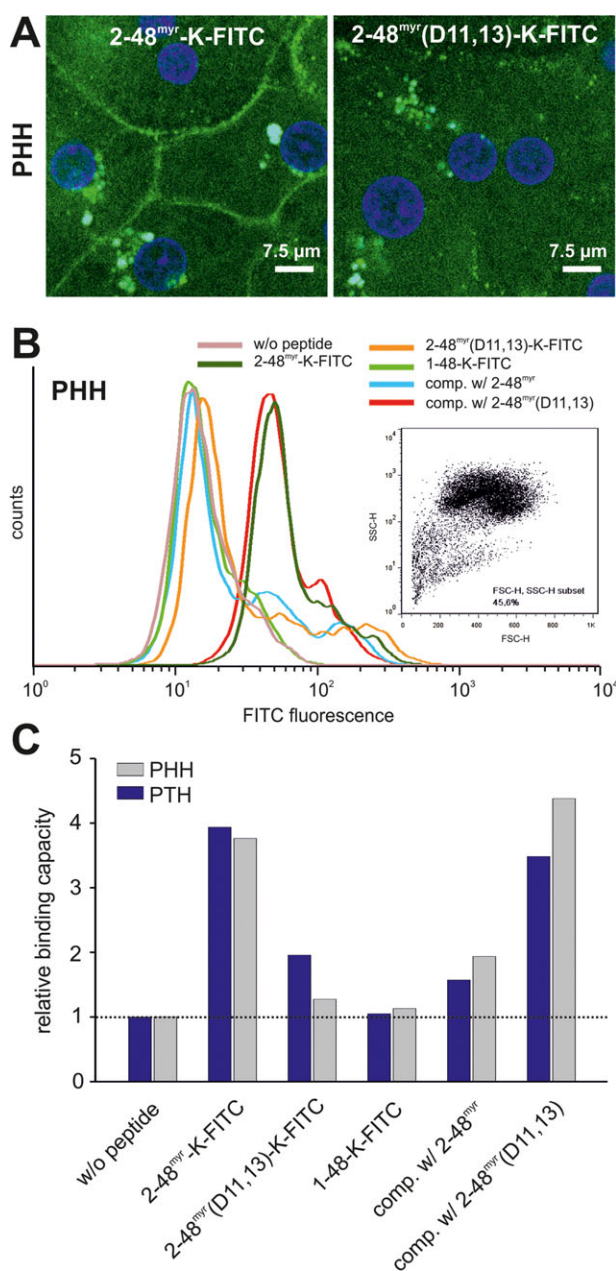


Fig. 2.

Fig. 2. HBVpreS/2-48<sup>myr</sup>-K-FITC binds HBV-susceptible PHH and PTH. (A) PHH were incubated for 30 minutes with 200 nM HBVpreS/2-48<sup>myr</sup>-K-FITC (2-48<sup>myr</sup>-K-FITC, left) or the mutant HBVpreS/2-48<sup>myr</sup>(D11,13)-K-FITC (2-48<sup>myr</sup>(D11,13)-K-FITC, right). After fixation, binding of the peptides was analyzed by confocal microscopy. Specific plasma membrane staining (green) was observed for 2-48<sup>myr</sup>-K-FITC but not for 2-48<sup>myr</sup>(D11,13)-K-FITC. Punctuated intracellular fluorescence derived by autofluorescence was also detectable in the absence of peptide (data not shown). Nuclei staining (DAPI) is shown in blue. (B) Flow cytometric analysis of peptide binding and binding competition. Cryopreserved PHH were incubated in solution with 200 nM FITC-labeled 2-48<sup>myr</sup>-K-FITC (dark green), 2-48<sup>myr</sup>(D11,13)-K-FITC (orange), or the nonmyristoylated peptide HBVpreS/1-48-K-FITC (1-48-K-FITC, light green). Autofluorescence of the cells is shown in pink (w/o peptide). Competition of binding was performed by incubating PHH with 200 nM FITC-labeled 2-48<sup>myr</sup>-K-FITC in the presence of a 100-fold excess (20 μM) of unlabeled HBVpreS/2-48<sup>myr</sup> (2-48<sup>myr</sup>, blue) or HBVpreS/2-48<sup>myr</sup>(D11,13) (2-48<sup>myr</sup>(D11,13), red). (C) Quantitative analysis of the experiment shown in (B) compared to a second binding assay performed with cryopreserved PTH. The relative binding capacities of both cell types were normalized by dividing the signal of peptide fluorescence through the respective signal caused by autofluorescence (w/o peptide).

HBV infection.<sup>29</sup> Unexpectedly, we observed the same sequence specific and myristoyl-dependent binding of HBVpreS/2-48<sup>myr</sup>-K-FITC to the PMH surface as for PHH, PTH, and HepaRG cells (Fig. 3A). Specific binding to PMH was confirmed by flow cytometry (data not shown). Binding was also detected in primary rat hepa-

toocytes (PRH) (Fig. 3B). Again, excess of unlabeled HBVpreS/2-48<sup>myr</sup> reduced the fluorescence to background level (blue line), whereas coinubation with HBVpreS/2-48<sup>myr</sup>(D11,13) had no effect (Fig. 3B, red line). Accordingly, an HBVpreS1-receptor is present on the hepatocytes of mice and rats. We extended this analysis and tested HBVpreS-peptide binding to primary hepatocytes from rabbits, dogs, cynomolgus monkeys, rhesus monkeys, and pigs. As depicted in Fig. 3C, we found specific binding of HBVpreS/2-48<sup>myr</sup>-K-FITC to rat, rabbit, and dog hepatocytes but surprisingly not to hepatocytes from cynomolgus and rhesus monkey, despite their closer evolutionary relation to humans. Binding was also not observed on pig hepatocytes. Thus, differentiated hepatocytes from some HBV nonsusceptible species do express the HBVpreS-specific receptor (mouse, rat, dog, and rabbit), while others do not (pig, cynomolgus, and rhesus monkey), indicating that a step downstream specific preS-binding must restrict HBV/HDV-infection in these species.

**HBVpreS-Receptor Expression Requires Hepatocyte Differentiation.** The susceptibility of HepaRG cells to HBV infection depends on a differentiated state of the cells.<sup>7,30</sup> Moreover, PHH lose their susceptibility to HBV when DMSO is withdrawn from the medium.<sup>31-34</sup> In order to test if this correlates with the presence of the HBVpreS-receptor we analyzed undifferentiated (5 days after seeding) and differentiated HepaRG cells (28 days after seeding, including a 2-week DMSO treatment) for their ability to bind HBVpreS/2-48<sup>myr</sup>-K-FITC. As seen in Fig. 4A (upper panel, left), HBVpreS/2-48<sup>myr</sup>-K-FITC did not stain the PM of undifferentiated cells, whereas binding was

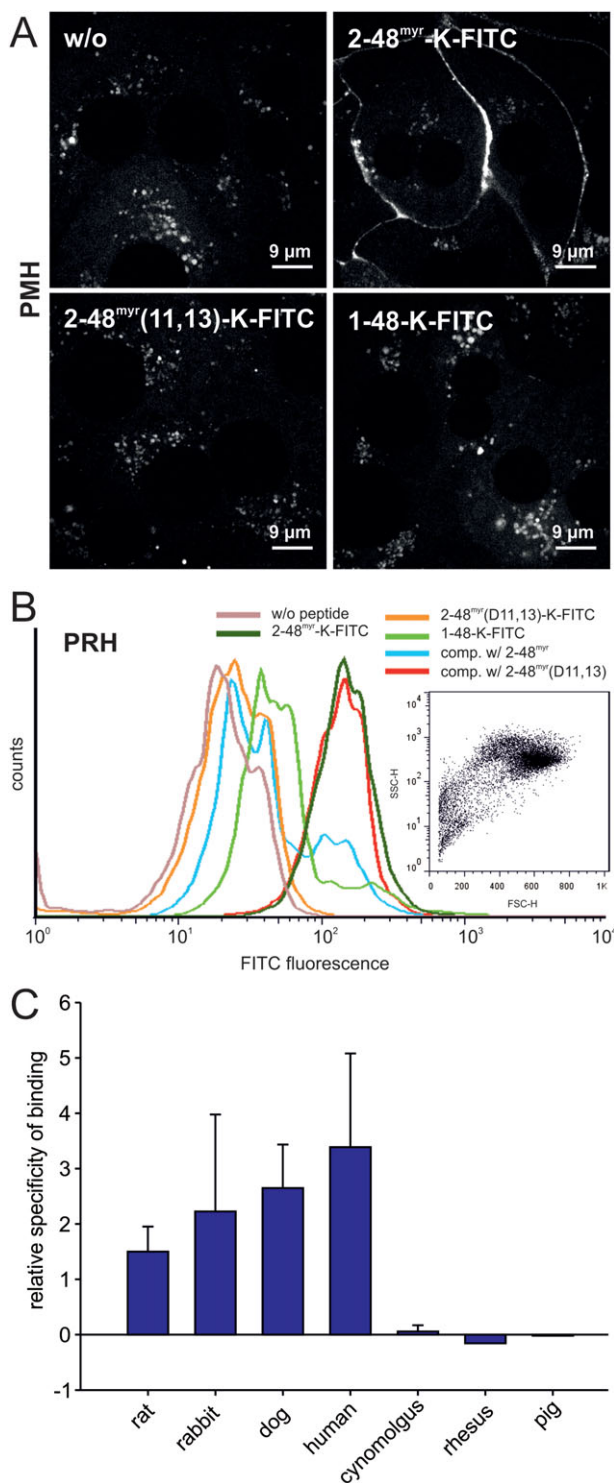


Fig. 3.

Fig. 3. HBVpreS/2-48<sup>myr</sup>-K-FITC specifically binds to primary hepatocytes of mouse, rat, rabbit, and dog. (A) Binding of fluorescently labeled peptides to PMH. PMH were incubated with 200 nM of HBVpreS/2-48<sup>myr</sup>-K-FITC (2-48<sup>myr</sup>-K-FITC, upper right), HBVpreS/2-48<sup>myr</sup>(D11,13)-K-FITC (2-48<sup>myr</sup>(D11,13)-K-FITC, lower left), and HBVpreS/1-48-K-FITC (1-48-K-FITC, lower right). After washing, cells were fixed with 4% PFA and analyzed by confocal microscopy. The autofluorescence of the cells in the absence of peptide (w/o) is depicted in the upper left panel. (B) Freshly isolated PRH were incubated with 200 nM of 2-48<sup>myr</sup>-K-FITC (dark green), 2-48<sup>myr</sup>(D11,13)-K-FITC (orange), or 1-48-K-FITC (light green). Binding competition was performed by coinubation of 200 nM 2-48<sup>myr</sup>-K-FITC in the presence of a 100-fold excess (20  $\mu$ M) of unlabeled HBVpreS/2-48<sup>myr</sup> (2-48<sup>myr</sup>, blue) or the mutant HBVpreS/2-48<sup>myr</sup>(D11,13) (2-48<sup>myr</sup>(D11,13), red). Fluorescence was quantified by flow cytometry. (C) Specific binding of 2-48<sup>myr</sup>-K-FITC to primary hepatocytes from various species. Cryopreserved rat, rabbit, dog, human, pig, cynomolgus, and rhesus monkey hepatocytes were incubated in suspension with 200 nM of the peptide and fluorescence was analyzed by flow cytometry. To exclude possible unspecific binding of the fatty acid residue (myr) we defined the ratio of 2-48<sup>myr</sup>-K-FITC to the mutant 2-48<sup>myr</sup>(D11,13)-K-FITC signal as the relative specificity of binding. Shown data represent two (rat, rabbit, dog), three (human, cynomolgus) or one (rhesus, pig) independent experiments.

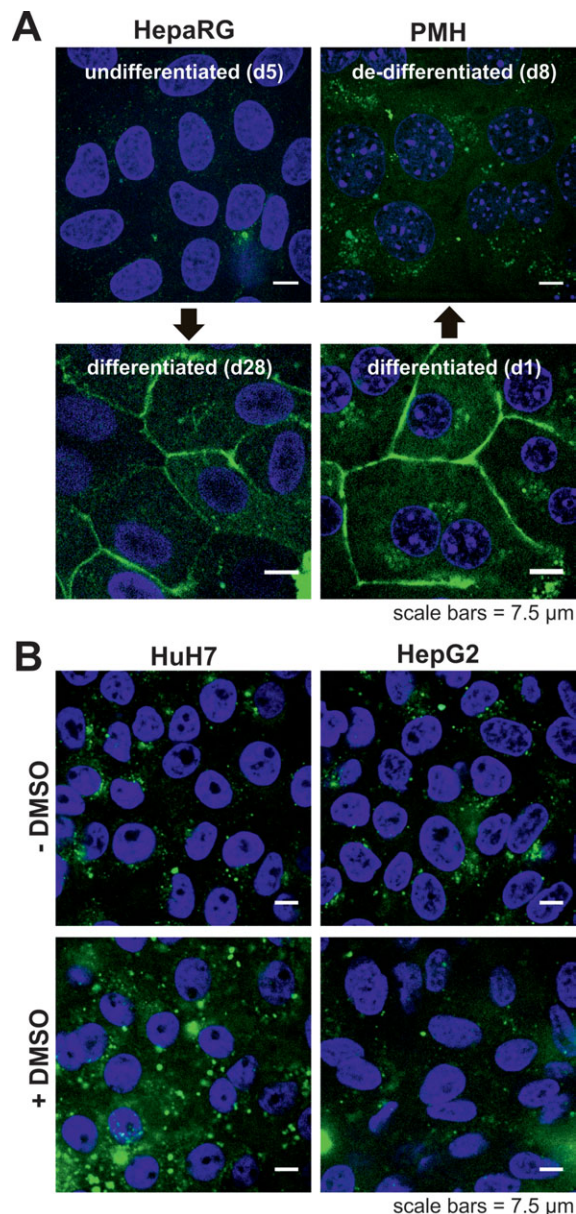


Fig. 4. Binding of HBVpreS/2-48<sup>myr</sup>-K-FITC depends on the differentiation state of the cell. (A) Undifferentiated (day 5 post plating, d5) and differentiated HepaRG cells (day 28 post plating and day 14 post-DMSO treatment, d28) were incubated with 200 nM of HBVpreS/2-48<sup>myr</sup>-K-FITC (left panels). PMH were incubated with the same peptide either in a differentiated state at day 1 post plating (diff. d1, lower right) or in a de-differentiated state after 8 days of cultivation without DMSO (de-diff. d8, upper right). Cells were washed, fixed with 4% PFA, and analyzed by confocal microscopy. Peptide-derived fluorescence is shown in green; nuclei were stained with DAPI (blue). (B) HuH7 and HepG2 cells are refractory to binding of HBVpreS/2-48<sup>myr</sup>-K-FITC. HuH7 (left panels) and HepG2 (right panels) hepatoma cells were incubated with 200 nM of HBVpreS/2-48<sup>myr</sup>-K-FITC either after having reached confluency (-DMSO, upper panels) or having been exposed to 2 weeks of DMSO-induced differentiation (+DMSO, lower panels). Cells were washed, fixed with 4% PFA, and analyzed by confocal microscopy. Peptide fluorescence is depicted in green; nuclei were stained with DAPI (blue). Note that even after DMSO-induced differentiation no specific staining at the plasma membrane of HepG2 and HuH7 cells could be observed.

seen after differentiation (lower panel, left). This implies a cell state-dependent induction of HBVpreS/2-48<sup>myr</sup>-receptor expression during HepaRG-differentiation. Accordingly, we investigated whether dedifferentiation of binding competent primary hepatocytes result in an opposite effect. We cultivated PMH in the absence of DMSO and followed their ability to bind HBVpreS/2-48<sup>myr</sup>-K-FITC over time (Fig. 4A, right panels). While freshly isolated PMH specifically accumulated the peptide at the PM, hepatocytes from the same preparation lost their ability to bind HBVpreS/2-48<sup>myr</sup>-K-FITC within a few days of cultivation. Loss of binding could be prevented by addition of DMSO (data not shown). This correlates with the fact that PHH lose their susceptibility for HBV during several days of cultivation in the absence of DMSO.<sup>28</sup> Thus, expression of an HBVpreS-receptor is linked to pathways controlling the differentiation state of hepatocytes.

To investigate whether HuH7 and HepG2 express detectable amounts of the HBVpreS-receptor following DMSO-induced differentiation, we performed binding experiments with these cells under differentiation conditions. As shown in Fig. 4B (upper panel) dividing cultures of HuH7 and HepG2 cells showed no significant binding of HBVpreS/2-48<sup>myr</sup>-K-FITC. Cultivation in the presence of 0.5% DMSO for 2 weeks did not render the cells competent for HBVpreS/2-48<sup>myr</sup>-K-FITC-binding (Fig. 4C, lower panels). Nonhepatoma cell lines with (293T, CHO-K1) or without a GAG-matrix (CHO-pgs745 cells) were also refractory for peptide binding (data not shown). This excludes a direct interaction with GAGs, a conclusion that was strengthened by the observation that binding of HBVpreS/2-48<sup>myr</sup>-K-FITC cannot be inhibited by heparin and suramin (Fig. 8A).

**Kinetics of the HBVpreS-Receptor Complex Formation and Stability.** To obtain insight into the kinetics of the HBVpreS-receptor complex-formation and its stability at the hepatocyte surface, we performed a time course of peptide-binding and release from the surface of PHH and PMH. As shown in Fig. 5A, association of HBVpreS/2-48<sup>myr</sup>-K-FITC with the PM proceeds rapidly. One minute after incubation of PHH with the peptide, the typical rim-like staining of the cell is detectable. The signal increases within ~20 minutes and remains virtually constant, indicating equilibrium. To examine kinetics of the peptide-receptor complex at the PM we incubated HBVpreS/2-48<sup>myr</sup>-K-FITC with PMH for 4 hours, removed the unbound peptide, and followed the disappearance of the membrane associated receptor/peptide complex for the duration of 24 hours at

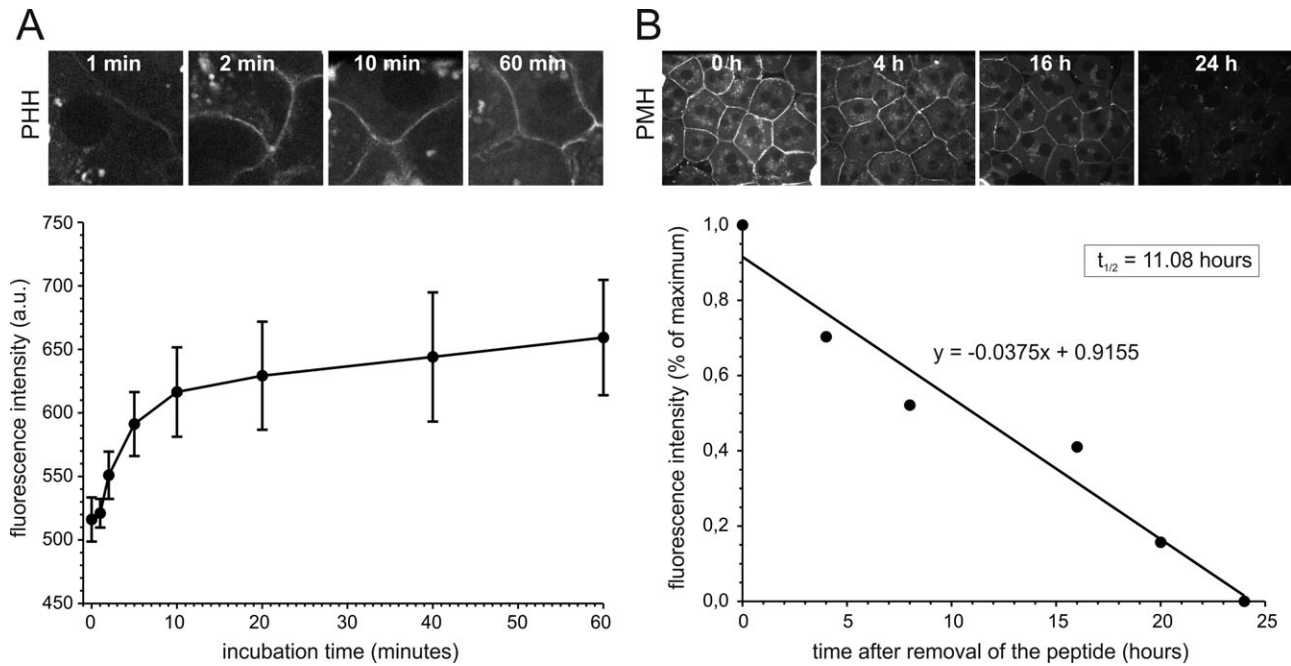


Fig. 5. Association and dissociation kinetics of HBVpreS/2-48<sup>myr</sup>-K-FITC to PHH and PMH (A) PHH were incubated for up to 60 minutes with HBVpreS/2-48<sup>myr</sup>-K-FITC. After 0, 1, 2, 5, 10, 20, 40, and 60 minutes, cells were washed and fixed with 4% PFA. Fluorescence was quantified on confocal images and plotted against the time (below). Representative pictures of peptide bound to the plasma membrane after 1, 2, 10, and 60 minutes are shown above. (B) PMH were incubated for 4 hours with 400 nM HBVpreS/2-48<sup>myr</sup>-K-FITC. 0, 4, 8, 16, 20, and 24 hours after peptide removal, cells were washed, supplied with fresh medium, and fixed with 4% PFA. Plasma membrane-associated fluorescence was quantified on confocal images and average fluorescence intensity at the respective points in time was plotted as the percentage of the maximum fluorescence (fluorescence after 0 hours) against the time. The half-life of the plasma membrane bound peptide was ~11 hours (below). Representative pictures from cells at 0, 4, 16, and 24 hours after peptide removal are depicted above.

37°C. Remarkably, fluorescence at the PM was still detectable 20 hours after removal of free peptide (Fig. 5B), indicating a very slow dissociation of the peptide from the receptor and a low turnover rate of the surface receptor. Quantification of the fluorescence revealed an approximate half-life of the peptide-receptor complex at the surface of PMH hepatocytes of about 11 hours (assuming that the FITC-label remains peptide associated). This is consistent with the *in vivo* half-life times in mice (Schieck et al.<sup>25</sup>).

To approximate the binding constant of the complex we incubated PMH with increasing concentrations of the wildtype and the mutant peptide and quantified cell-associated fluorescence by flow cytometry. HBVpreS/2-48<sup>myr</sup>-K-FITC, but also the mutant HBVpreS/2-48<sup>myr</sup>(D11,13)-K-FITC showed a concentration-dependent increase of cell-associated fluorescence (Fig. 6A). However, the binding curves differed considerably at concentrations below 400 nM. While the wildtype peptide showed significant binding, the mutant peptide was barely associated with the cells. At higher concentrations (400 nM to 3.2  $\mu$ M), a linear increase of cell-associated fluorescence was observed for both peptides. Since non-myristoylated HBVpreS/1-48-

K-FITC did not exhibit significant cell association even at the highest concentration (3.2  $\mu$ M), we conclude that binding of the mutant peptide is driven by a myristoyl-mediated, unspecific PM-interaction. By subtraction of the values from nonspecific HBVpreS/2-48<sup>myr</sup>(D11,13)-K-FITC-binding from the signal of HBVpreS/2-48<sup>myr</sup>-K-FITC-binding we obtained a specific saturation binding curve (Fig. 6B). To estimate the dissociation constant  $K_D$  of the complex, we plotted the ratio of the concentrations of bound ligand/free ligand against the fluorescence intensity (by Scatchard plot, Fig. 6C). Assuming a first-order binding kinetics, we obtained a  $K_D$  of ~67 nM at room temperature. This value neglects a possible turnover of the receptor and the peptide (by e.g., endocytosis or peptide degradation).

**HBVpreS-Receptor Complex on Hepatocytes Shows No Detectable Lateral Movement.** We sublocalized the peptide-receptor complex on the cell surface and analyzed its ability to laterally move within the membrane by using laser scanning confocal live cell imaging. To quantify the dynamics of peptide-associated fluorescence we photobleached a region within the focal plane of the PM of PMH and



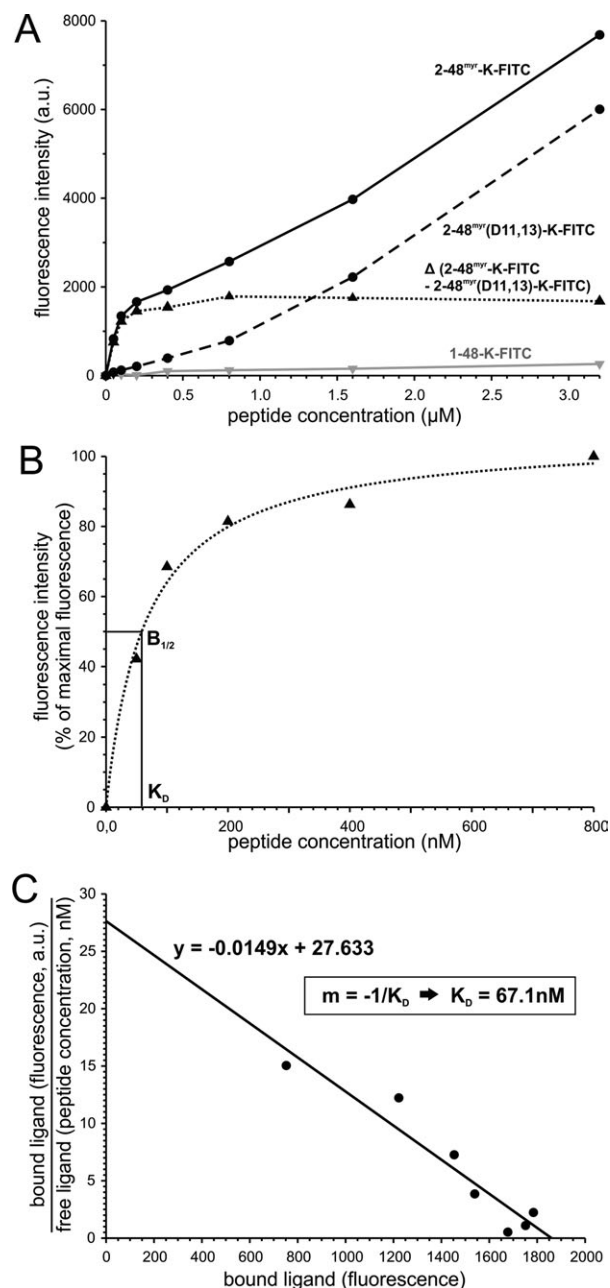


Fig. 6. Determination of the dissociation constant of the HBVpreS-receptor complex on PMH. (A) Freshly isolated PMH were incubated with increasing concentrations of HBVpreS/2-48<sup>myr</sup>-K-FITC (2-48<sup>myr</sup>-K-FITC, solid line), HBVpreS/2-48<sup>myr</sup>(D11,13)-K-FITC (2-48<sup>myr</sup>(D11,13)-K-FITC, dashed line), and HBVpreS/1-48-K-FITC (1-48-K-FITC, gray solid line) as described. Fluorescence intensity was quantified by flow cytometry and plotted against the peptide concentration. Unspecific binding at higher concentrations was observed with both 2-48<sup>myr</sup>-K-FITC and the mutant peptide, and is probably caused by interactions of the membrane with the fatty acid moiety. Therefore, unspecific binding was subtracted from the binding curve of 2-48<sup>myr</sup>-K-FITC resulting in a specific and saturable binding curve (dotted line). (B) Normalized values obtained from the binding analysis shown in (A) (dotted line) were used to calculate the dissociation constant ( $K_0$ ) by nonlinear regression analysis. Fluorescence intensity is shown as percentage of the maximal fluorescence (fluorescence intensity at 800 nM). (C) Scatchard plot analysis from the data obtained, resulting in a  $K_0$  of  $\sim 67$  nM.

measured fluorescence recovery over time (FRAP). Instead of an FITC-labeled peptide we applied HBVpreS/2-48<sup>myr</sup>-C-Atto565, a peptide bearing the more photostable Atto565 fluorophore. As depicted in Fig. 7A (upper panel) the peptide-associated fluorescence was detectable at the microvilli of hepatocytes 4 seconds before photobleaching. No recovery was observed within 30 seconds after bleaching (right pictures). In contrast, carbocyanine DiI, which incorporates into the fluid-phase lipid bilayer, showed fluorescence recovery within 6 seconds (Fig. 7A, lower panel). Hence, the HBVpreS1-receptor complex does not show lateral movement within the PM. We further analyzed the sublocalization of the peptide at the PM of PRH by confocal microscopy. Following incubation with 200 nM HBVpreS/2-48<sup>myr</sup>-K-FITC, a Z-stack projection confirmed marginal staining in intracellular cell compartments (Fig. 7B). Since the lack of lateral movement of the peptide receptor complex indicates a possible association with the actin cytoskeleton we performed a colocalization experiment using HBVpreS/2-48<sup>myr</sup>-K-FITC (green) and Phalloidin-Alexa546, a specific label for F-actin (red). As depicted in Fig. 7C, a subpopulation of F-actin colocalized with the peptide, seen as yellow spots surrounded by peptide-clusters.

**HBVpreS/2-48<sup>myr</sup>-K-FITC Binds to a Proteinacious Molecule, Independently of Glycosamino Glycans.** Since HBV and HDV infection are efficiently inhibited by highly sulfated agents like heparin and suramin, we tested whether they also interfere with peptide binding. As shown in Fig. 8A, HBVpreS/2-48<sup>myr</sup>-K-FITC binds PMH in the presence of 600  $\mu\text{g}/\text{mL}$  heparin or 200  $\mu\text{g}/\text{mL}$  suramin, concentrations that inhibit HBV and HDV infection. Thus, the peptide does not address glycosaminoglycans as a possible target. However, the HBVpreS-receptor complex on PMH was partially sensitive to the treatment with the two proteases trypsin or GluC, indicating a possible involvement of a proteinacious molecule in the recognition of the peptidic ligand.

## Discussion

Up to now there is only limited experimental evidence to explain two notable features of an HBV infection: (1) the restriction to infect only differentiated hepatocytes and (2) the species specificity, limiting HBV infections to humans and chimpanzees. We here tested the hypothesis if both aspects of HBV infection may be linked to a specific interaction of the N-terminal preS1-domain. We took advantage of a fluorescently labeled inhibitory preS1-lipopeptide (HBVpreS/2-48<sup>myr</sup>-K-FITC)

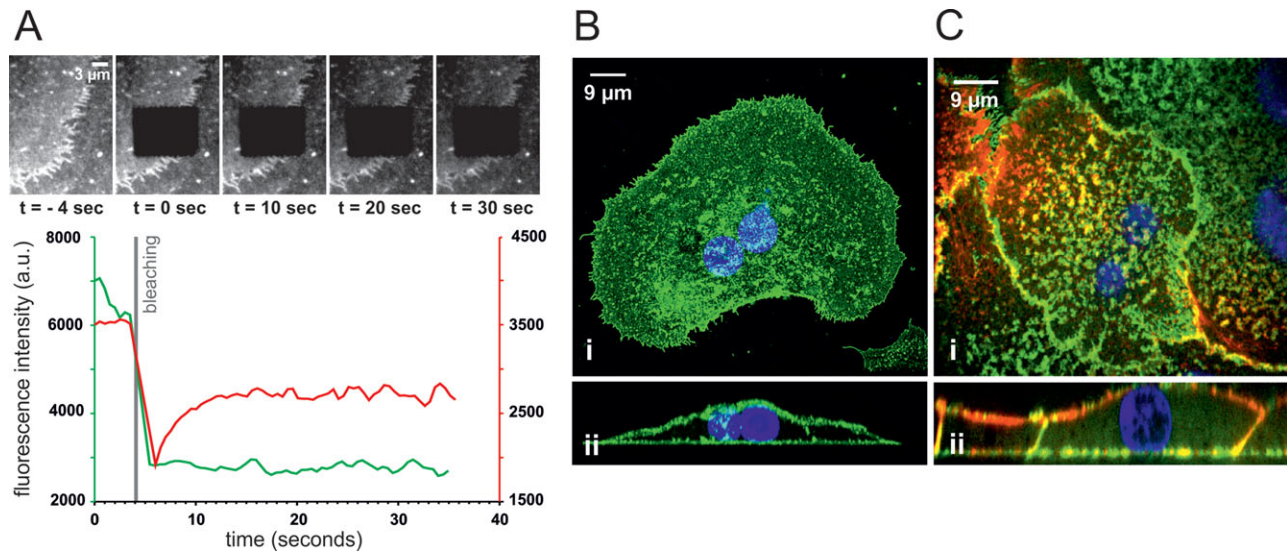


Fig. 7. Lateral diffusion capability and localization of peptide-receptor complexes on the plasma membrane. (A) PMH were incubated with 400 nM HBVpreS/2-48<sup>myr</sup>-C-Atto565, washed, and analyzed using a confocal live-cell imaging setup. Time-lapse experiments were performed following laser photobleaching of a specified region (black rectangles in the confocal images above) for 4 seconds. FRAP was recorded for 30 seconds. The graph depicts a representative FRAP experiment with cells incubated with HBVpreS/2-48<sup>myr</sup>-C-Atto565 (green line), and cells stained with Dil, a membrane motile dye that was used as control (red line). (B) Plasma membrane specific localization of HBVpreS/2-48<sup>myr</sup>-K-FITC on PRH, detected by confocal microscopy. PRH were incubated with 200 nM HBVpreS/2-48<sup>myr</sup>-K-FITC, fixed, and analyzed by confocal microscopy. Shown are the maximum projection (i), and a side view (ii) of a reconstructed Z-stack. Images were deconvolved before reconstruction. The pictures demonstrate a patterned binding, predominantly at the plasma membrane and not in intracellular compartments. (C) Colocalization of receptor-bound HBVpreS/2-48<sup>myr</sup>-K-FITC with the actin cytoskeleton in PRH. Cells were incubated with HBVpreS/2-48<sup>myr</sup>-K-FITC (green), fixed, and the actin cytoskeleton was stained with Phalloidin-Alexa546 (red). Colocalization of bound peptide and actin is seen as yellow spots, with actin surrounded by peptide clusters.

(Fig. 1B), thus allowing visual tracing of the HBVpreS/receptor complex. HBVpreS/2-48<sup>myr</sup>-K-FITC associates within minutes to the PM of differentiated hepatocytes (Fig. 5) in a sequence- and myristoyl-dependent manner (Fig. 1C). In contrast to the control peptide, which displays only unspecific cell association via its fatty acid moiety, specific binding of HBVpreS/2-48<sup>myr</sup>-K-FITC was detectable with a calculated  $K_D$  of 67 nM. Unexpectedly, binding was not restricted to HBV-susceptible cells like PHH, PTH, or HepaRG cells (Fig. 2) but was also evident in hepatocytes from mouse, rat, rabbit, and dog, although slight differences were observed (Fig. 3). A remarkable observation was the absence of specific receptor sites in hepatocytes from pigs, cynomolgus, and rhesus monkeys. Together with the *in vivo* data showing that cynomolgus monkeys fail to accumulate the HBVpreS peptide in the liver (Schieck et al.<sup>25</sup>), this suggests the lack of a functional HBV receptor in this species.

The species-specific binding capabilities determined *in vitro* strongly support the selective liver accumulation of only those peptides that are able to inhibit HBV infection (Schieck et al.<sup>25</sup>). Our finding that a number of HBV nonsusceptible hepatocytes bind the HBVpreS-peptide suggests that the refractiveness to infection of these cells is not caused by the absence of a binding

competent receptor. Since rodent cells support appropriate assembly and secretion of HBV following transfection, the block of infection must be linked to a post-binding host factor activity (fusion) or related to a postfusion step (transport, DNA-repair), or both. These possibilities have to be analyzed in the future and will have important implications for the development of small animal models for HBV and HDV.

Tight and specific binding required both, the N-terminal myristoylation of the preS1-sequence, probably mediating close contact and correct positioning of the peptide at the hepatocyte membrane, and the integrity of a highly conserved central sequence motif 9-NPLGFFP-15 flanked by two short amino acid stretches. Binding occurs only in hepatic cells that either accomplished a highly differentiated state or are kept under conditions to stabilize such a state. HuH7 and HepG2 cell lines did not bind HBVpreS-lipopeptides, either in a dividing, asynchronous culture, or in a DMSO-treated differentiated state. This might explain their refractiveness against HBV/HDV infection. Since these cell lines are derived from liver tumors, it would stand to reason that during the transformation process of hepatocytes HBV receptor expression might get lost. Since the requirement for a resting state of the hepatocyte to uphold susceptibility to infection is a general

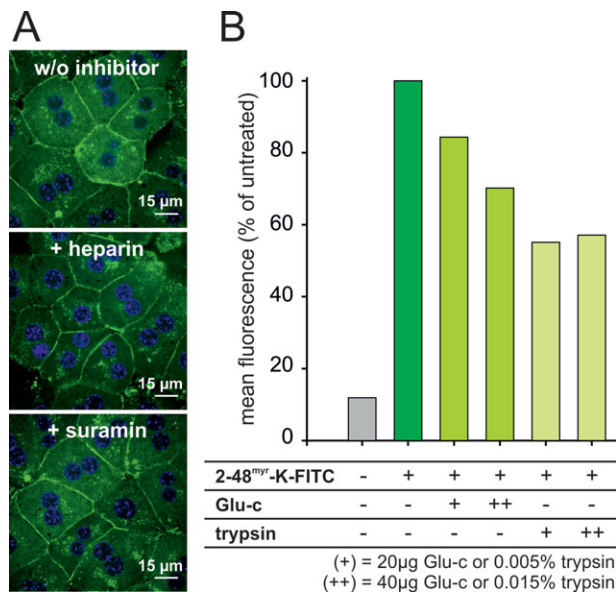


Fig. 8. HBVpreS/2-48<sup>myr</sup>-K-FITC binding is sensitive to proteases and cannot be inhibited by heparin and suramin. (A) PMH were incubated with 200 nM of HBVpreS/2-48<sup>myr</sup>-K-FITC in the absence or presence of heparin (600 µg/mL) or suramin (200 µg/mL). These concentrations are known to inhibit HBV infection. FITC fluorescence (green) and DAPI-stained nuclei (blue) are shown on the confocal images. Note that both infection inhibitors do not interfere with peptide binding. (B) Binding capability of PMH after protease treatment. PMH were pretreated with the indicated concentrations of the proteases Glu-C and trypsin, washed, and incubated with 200 nM HBVpreS/2-48<sup>myr</sup>-K-FITC. Cells were washed and cell-associated fluorescence was measured by flow cytometry. Mean fluorescence is shown as the percentage of fluorescence in the mock-treated control.

feature of hepadnaviruses, it is possible that hepatocyte-specific binding of both, ortho- and avihepadnaviruses, is also mediated by their N-terminal preS-domains. It is noteworthy that a commonly accepted but rarely scrutinized observation already hinted at the possibility that HBV receptor expression is not limited to hepatocytes from human primates: The finding that *Tupaia belangeri*, a member of the scandentia, is susceptible to HBV and that infection of PTH is blocked by HBVpreS lipopeptides,<sup>20</sup> suggested the existence of such an entry receptor in tupaia. Binding of the peptide to PTH (Fig. 2C) confirms this hypothesis.

Regarding the future clinical application of Myrcludex B, the lead substance of HBVpreS lipopeptides, a medically important finding was that the  $K_D$  (~67 nM) differed by a factor >50 from the median inhibitory concentration ( $IC_{50}$ ) determined in infection inhibition assays. This raises the question of whether we address the same molecule in these assays. However, the strong correlation of the inhibition activity of more than 25 peptide mutants<sup>21</sup> with their ability to target the HBVpreS-receptor *in vivo* (Schieck et al.<sup>25</sup>) makes the assumption highly unlikely. We therefore

hypothesize that partial occupation of binding-sites already functionally inactivates the receptor. Thus, HBV, like other enveloped viruses, may require a receptor multimerization. Blocking of a single subunit by the peptide might therefore be sufficient to perturb entry. Since we did not detect significant lateral movement of the peptide-receptor complex (Fig. 7), we further suggest receptor association with the actin microfilaments. The partial sensitivity of the receptor ligand complex against the two proteases trypsin and GluC (Fig. 8B) indicates a proteinaceous nature.

While the myristoylated peptide binds to hepatocytes within minutes, only a minor fraction of HBV infects PHH within 12 hours. This discrepancy might be explained by a hidden N-terminal preS-domain of L-protein in the virion followed by an only slow transition from the viral into the PM of hepatocytes (Supporting Fig. 1). This probably occurs very close to or even within the hepatocyte surface. Thus, the peptide might be regarded as a constitutively active ligand.

Taken together, the characterization of the hepatocyte-specific preS-receptor complex will allow narrowing down reasonable receptor candidates, which is important with respect to the future development of immune-competent animal models of HBV.

**Acknowledgment:** We thank Martina Spille for excellent technical assistance, Christoph Leder for initial help with the flow cytometry studies, Thomas Müller for peptide synthesis, Maura Dandri for providing primary hepatocytes from *Tupaia belangeri*, and Alexander Alexandrov for stimulating discussions. We thank Ulrike Engel and Christian Ackermann from the Nikon Imaging Center, Heidelberg, for excellent technical support in microscopy. We thank Ralf Bartenschlager for continuous intellectual support.

## References

- Lok AS. Prevention of hepatitis B virus-related hepatocellular carcinoma. *Gastroenterology* 2004;127(5 Suppl 1):S303-S309.
- Hoofnagle JH, Doo E, Liang TJ, Fleischer R, Lok AS. Management of hepatitis B: summary of a clinical research workshop. *HEPATOLOGY* 2007;45:1056-1075.
- Ganem D, Prince AM. Hepatitis B virus infection—natural history and clinical consequences. *N Engl J Med* 2004;350:1118-1129.
- Bruss V. Hepatitis B virus morphogenesis. *World J Gastroenterol* 2007;13:65-73.
- Lu X, Block TM, Gerlich WH. Protease-induced infectivity of hepatitis B virus for a human hepatoblastoma cell line. *J Virol* 1996;70:2277-2285.
- Glebe D, Urban S. Viral and cellular determinants involved in hepadnaviral entry. *World J Gastroenterol* 2007;13:22-38.
- Gripon P, Rumin S, Urban S, Le SJ, Glaise D, Canine I, et al. Infection of a human hepatoma cell line by hepatitis B virus. *Proc Natl Acad Sci U S A* 2002;99:15655-15660.

8. Walter E, Keist R, Niederost B, Pult I, Blum HE. Hepatitis B virus infection of tupaia hepatocytes in vitro and in vivo. *HEPATOLOGY* 1996; 24:1-5.
9. Leistner CM, Gruen-Bernhard S, Glebe D. Role of glycosaminoglycans for binding and infection of hepatitis B virus. *Cell Microbiol* 2008;10: 122-133.
10. Schulze A, Gripon P, Urban S. Hepatitis B virus infection initiates with a large surface protein-dependent binding to heparan sulfate proteoglycans. *HEPATOLOGY* 2007;46:1759-1768.
11. Bruss V, Hagelstein J, Gerhardt E, Galle PR. Myristylation of the large surface protein is required for hepatitis B virus in vitro infectivity. *Virology* 1996;218:396-399.
12. Gripon P, Le SJ, Rumin S, Guguen-Guillouzo C. Myristylation of the hepatitis B virus large surface protein is essential for viral infectivity. *Virology* 1995;213:292-299.
13. LeSeyec J, Chouteau P, Cannie I, Guguen-Guillouzo C, Gripon P. Infection process of the hepatitis B virus depends on the presence of a defined sequence in the pre-S1 domain. *J Virol* 1999;73:2052-2057.
14. Blanchet M, Sureau C. Infectivity determinants of the hepatitis B virus pre-S domain are confined to the N-terminal 75 amino acid residues. *J Virol* 2007;81:5841-5849.
15. LeSeyec J, Chouteau P, Cannie I, Guguen-Guillouzo C, Gripon P. Role of the pre-S2 domain of the large envelope protein in hepatitis B virus assembly and infectivity. *J Virol* 1998;72:5573-5578.
16. Ni Y, Sonnabend J, Seitz S, Urban S. The pre-s2 domain of the hepatitis B virus is dispensable for infectivity but serves a spacer function for L-protein-connected virus assembly. *J Virol* 2010;84:3879-3888.
17. Abou-Jaoudé G, Sureau C. Entry of hepatitis delta virus requires the conserved cysteine residues of the hepatitis B virus envelope protein antigenic loop and is blocked by inhibitors of thiol-disulfide exchange. *J Virol* 2007;81:13057-13066.
18. Schelhaas M, Malmstrom J, Pelkmans L, Haugstetter J, Ellgaard L, Grunewald K, et al. Simian Virus 40 depends on ER protein folding and quality control factors for entry into host cells. *Cell* 2007;131:516-529.
19. Glebe D, Aliakbari M, Krass P, Knoop EV, Valerius KP, Gerlich WH. Pre-s1 antigen-dependent infection of Tupaia hepatocyte cultures with human hepatitis B virus. *J Virol* 2003;77:9511-9521.
20. Glebe D, Urban S, Knoop EV, Cag N, Krass P, Grun S, et al. Mapping of the hepatitis B virus attachment site by use of infection-inhibiting preS1 lipopeptides and tupaia hepatocytes. *Gastroenterology* 2005;129: 234-245.
21. Schulze A, Schieck A, Ni Y, Mier W, Urban S. Fine mapping of pre-S sequence requirements for hepatitis B virus large envelope protein-mediated receptor interaction. *J Virol* 2010;84:1989-2000.
22. Petersen J, Dandri M, Mier W, Lutgehetmann M, Volz T, von WF, et al. Prevention of hepatitis B virus infection in vivo by entry inhibitors derived from the large envelope protein. *Nat Biotechnol* 2008;26:335-341.
23. Barrera A, Guerra B, Norvall L, Lanford RE. Mapping of the hepatitis B virus pre-S1 domain involved in receptor recognition. *J Virol* 2005; 79:9786-9798.
24. Gripon P, Cannie I, Urban S. Efficient inhibition of hepatitis B virus infection by acylated peptides derived from the large viral surface protein. *J Virol* 2005;79:1613-1622.
25. Schieck A, Schulze A, Gähler C, Müller T, Haberkorn U, Alexandrov A, et al. Hepatitis B virus hepatotropism is mediated by specific receptor recognition in the liver and not restricted to susceptible hosts. *HEPATOLOGY* 2013;58:43-53.
26. Weiss TS, Pahernik S, Scheruebl I, Jauch KW, Thasler WE. Cellular damage to human hepatocytes through repeated application of 5-aminolevulinic acid. *J Hepatol* 2003;38:476-482.
27. Seglen PO. Preparation of isolated rat liver cells. *Methods Cell Biol* 1976;13:29-83.
28. Gripon P, Diot C, Theze N, Fourel I, Loreal O, Brechot C, et al. Hepatitis B virus infection of adult human hepatocytes cultured in the presence of dimethyl sulfoxide. *J Virol* 1988;62:4136-4143.
29. Dandri M, Burda MR, Torok E, Pollok JM, Iwanska A, Sommer G, et al. Repopulation of mouse liver with human hepatocytes and in vivo infection with hepatitis B virus. *HEPATOLOGY* 2001;33:981-988.
30. Schulze A, Mills K, Weiss TS, Urban S. Hepatocyte polarization is essential for the productive entry of the hepatitis B virus. *HEPATOLOGY* 2012;55:373-383.
31. Gripon P, Diot C, Corlu A, Guguen-Guillouzo C. Regulation by dimethylsulfoxide, insulin, and corticosteroids of hepatitis B virus replication in a transfected human hepatoma cell line. *J Med Virol* 1989;28: 193-199.
32. Gripon P, Diot C, Guguen-Guillouzo C. Reproducible high level infection of cultured adult human hepatocytes by hepatitis B virus: effect of polyethylene glycol on adsorption and penetration. *Virology* 1993;192: 534-540.
33. Rumin S, Gripon P, Le SJ, Corral-Debrinski M, Guguen-Guillouzo C. Long-term productive episomal hepatitis B virus replication in primary cultures of adult human hepatocytes infected in vitro. *J Viral Hepat* 1996;3:227-238.
34. Ozer A, Khaoustov VI, Mearns M, Lewis DE, Genta RM, Darlington GJ, et al. Effect of hepatocyte proliferation and cellular DNA synthesis on hepatitis B virus replication. *Gastroenterology* 1996;110:1519-1528.